Performance evaluation and comparison of spatial modulation and non-DC MIMO *m*-CAP techniques in an indoor VLC system

Mahdi Nassiri[1], Saeed Ashouri[1], Gholamreza Baghersalimi[1]✉, and Zabih Ghassemlooy[2]

[1]Department of Electrical Engineering, University of Guilan, Rasht, Iran
[2]Optical Communications Research Group, Faculty of Engineering and Environment, Northumbria University, Newcastle, UK

✉ Email: bsalimi@guilan.ac.ir

Abstract: In this paper, we propose and apply two novel schemes of multi-band carrierless amplitude and phase (*m*-CAP) modulation for spatial modulation (SM) based visible light communications (VLC) systems. In SM, both spatial and signal constellation are utilised to improve the performance of the *m*-CAP system. Here, we have adopted the non-DC *m*-CAP which is a power efficient technique with no DC-bias. The bit error rate (BER) performance and the spectral efficiency of the proposed systems are compared with single-input single-output (SISO) and multiplexing multiple-input multiple-output (MIMO) *m*-CAP systems. Results demonstrate that non-DC *m*-CAP, with the same spectral efficiency as that of SISO *m*-CAP, outperforms other schemes in terms of BER due to its power efficiency, however a higher spectral efficiency can be achieved by the SM-MIMO *m*-CAP scheme.

1. Introduction

The radio frequency (RF) band is regarded as the most popular section of the electromagnetic spectrum for communication purposes, which establishes links with a wider coverage area and higher mobility at the cost of reduced level of security at the physical layer and lower data rates. However, due to the rapid growth of wireless network traffic and the need for sufficient bandwidth to provide high data rates, the current available RF spectrum is facing what is known as the spectral congestion [1].

Recently, visible light communications (VLC), as an alternative complementary technology to RF wireless technologies, has earned the attention of researchers to address the bandwidth bottleneck due to its ability to provide both illumination and data communications at high speeds (i.e., order of magnitude higher than RF) by using white light emitting diodes (LEDs) [2]. There are two main types of white LEDs that are used as light sources. The blue LED with yellow phosphor coating, which is the most popular due to its uniform illumination profile and cost efficiency. Although, due to the slow response of the phosphor, it has a limited bandwidth in the range of a few MHz. The RGB (red-green-blue) LED, which employs a mixture of three separate coloured LEDs to generate white light. This LED offers higher modulation bandwidth, but colour balancing is still an issue [3].

An interesting approach to overcome the bandwidth limitation of LEDs is the use of orthogonal frequency-division multiplexing (OFDM), which offers high spectral efficiency, η_{se}, and enables utilisation of power and bit loading. However, due to the intrinsic high peak-to-average power ratio (PAPR) of OFDM and a limited linear range of the LED power-current response, nonlinear distortion can degrade the performance of the VLC system [4].

Recently, an alternative approach known as carrierless amplitude and phase (CAP) modulation has been proposed for VLC, which outperforms OFDM in terms of data rate under the same test conditions [5]. Furthermore, unlike OFDM in CAP there is no need for fast Fourier transform (FFT) and inverse fast Fourier transform (IFFT). The carrier frequencies in CAP are generated by using the cost-efficient and simple finite impulse response (FIR) filters, which reduce the complexity of the VLC system. Additionally, PAPR of CAP systems is lower than that of OFDM, thus it is more robust against nonlinearity of the LEDs. Despite advantages of CAP, it has some limitations such as a fixed modulation order, which prohibits the use of bit loading technique, and the requirement for a flat channel, which is available in VLC systems [4, 6].

To address the previous limitations in CAP, multi-band CAP (*m*-CAP) for fibre-optic communications was proposed in [7], in which the gross signal bandwidth is split into *m* equally spaced subcarriers (SCs) to relax the need for a flat channel in RF systems. The results have demonstrated that *m*-CAP outperforms CAP in terms of bandwidth efficiency, dispersion and data rate. In [6, 8], *m*-CAP was employed for VLC with η_{se} of 4.85 b/s/Hz (i.e., a bitrate of 31.53 Mb/s) for ten SCs (i.e., m = 10). Nevertheless, increasing *m* leads to significant increase in the complexity of system due to the requirement of more FIR filters at both the transmitter (Tx) and the receiver (Rx).

In order to achieve higher data rates in *m*-CAP systems, the multiple-input multiple-output (MIMO) technique have also been investigated recently. In [9], a MIMO technique for CAP VLC employing repetition coding (RC) and spatial diversity was proposed to improve the bit error rate (BER) performance and η_{se}. In [9] it was shown that, in the case of uncorrelated VLC channels, spatial multiplexing outperforms the RC method. Furthermore, an experimental investigation of multiplexing MIMO for *m*-CAP VLC systems was reported in [10] with a maximum data rate of 249 Mbps for the best case.

Another MIMO technique known as optical spatial modulation (OSM) was proposed in [11, 12], where both spatial and signal constellations were exploited to achieve higher η_{se} compared to other techniques. In this method, only one LED is used at a time, so that the index of the transmitting

LED also conveys information. At the Rx, spatial demodulator estimates the index of the active LED based on the received signal power. In addition, in [13] a novel combination of OSM and OFDM was adopted to eliminate the need for a DC-bias. In this method, the positive and negative signals were assigned to LEDs 1 and 2, respectively, where only a single LED is on at a given time. It was shown that, non-DC OFDM offered improved power efficiency compared to DC-biased optical OFDM (DCO-OFDM) and asymmetrically clipped optical OFDM (ACO-OFDM) for the same η_{se}.

In [8], an experimental implementation of both CAP and *m*-CAP VLC over a transmission span of 1 m was reported showing a bitrate of 9 Mb/s, ~24 Mb/s and ~31 Mb/s for 1, 4 and 8 SCs, respectively. In this research, for the signal and the LED bandwidth of 6.5 MHz and 4.5 MHz, respectively, the achieved η_{se} for 1, 4 and 8 SCs were 1.4 b/s/Hz, 3.6 b/s/Hz and 4.7 b/s/Hz, respectively. In [6], a common CAP signal was divided into 2, 4, 6, 8 and 10 SCs and was shown that for a given total bandwidth of 6.5 MHz and for 10 SCs, a bitrate of 31.53 Mb/s or an η_{se} of 4.85 b/s/Hz was achievable. However, increasing the number of SCs leads to increased number of FIR filters on both the Tx and Rx, which results in a significant increase in computational complexity. In [10], both of space and frequency multiplexing were used to enhance the transmission speed of the *m*-CAP VLC system. A 4×4 MIMO VLC system based on *m*-CAP was experimentally carried out to this end. The reported overall data rate was ~249 Mb/s for m = 20 and a total bandwidth of 20 MHz while the link span and the target BER were 1 m and 10^{-3}, respectively.

To the best of author's knowledge, in this paper we report for the first time spatial modulation (SM) and non-DC MIMO techniques for *m*-CAP VLC. We compare the BER performance and η_{se} of the proposed scheme with single-input single-output (SISO) and multiplexing MIMO *m*-CAP systems.

The rest of this paper is organised as follows. In Section II principles of the *m*-CAP and the VLC subsystem are discussed followed by introduction of SISO, multiplexing MIMO, SM and non-DC *m*-CAP. In Section III significant results are presented and discussed. Finally, Section IV is devoted to the conclusions.

2. System setup

2.1. Principles of the m-CAP system

Fig. 1 shows the block diagram of the *m*-CAP modulator and demodulator. At first, m independent pseudo-random binary sequences D_1 - D_m are generated for each m SCs. These data streams are then mapped into M-quadrature amplitude modulation (M-QAM) complex symbols according to the corresponding order ranging from M_1 to M_m. Next, up-sampling is carried out by inserting $n_s - 1$ zeros between two successive complex symbols. The up-sampling factor is given as [14]

$$n_s = \lceil 2m(1+\beta) \rceil, \tag{1}$$

where $\lceil . \rceil$ is the ceiling function, and β is the roll-off factor of square root raised cosine (SRRC) filter. The up-sampled complex symbols are then split into real and imaginary components in each branch, which are then applied to the in-phase and quadrature SRRC filters, respectively. Note that, FIR filters are defined as the product of the SRRC filter and sine and cosine signals for in-phase and quadrature, respectively, which are given by [15]

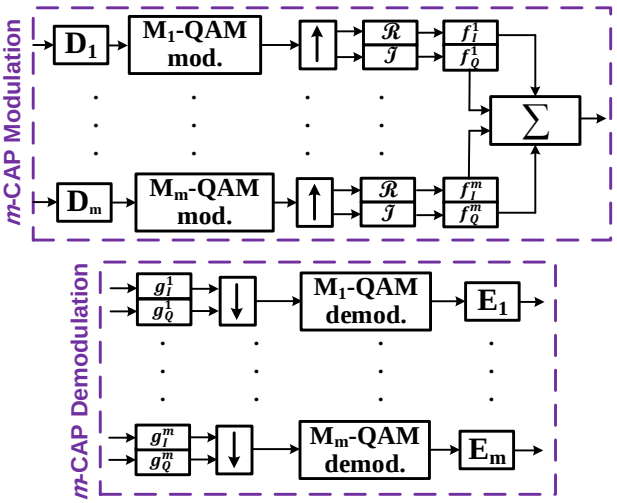

Fig. 1. *Block diagram of m-CAP modulator and demodulator*

$$f_I^{\,m}(t) = \left[\frac{\sin\left[\gamma(1-\beta)\right] + 4\beta \frac{t}{T_s}\cos\left[\gamma\delta\right]}{\gamma\left[1-\left(4\beta\frac{t}{T_s}\right)^2\right]} \right] . \cos\left[\gamma(2m-1)\delta\right], \tag{2}$$

$$f_Q^{\,m}(t) = \left[\frac{\sin\left[\gamma(1-\beta)\right] + 4\beta \frac{t}{T_s}\cos\left[\gamma\delta\right]}{\gamma\left[1-\left(4\beta\frac{t}{T_s}\right)^2\right]} \right] . \sin\left[\gamma(2m-1)\delta\right], \tag{3}$$

where T_s is the symbol duration, $\gamma = \pi t / T_s$ and $\delta = 1+\beta$. Assuming that, the up-sampled in-phase and quadrature components of the n^{th} branch as $s_I^n(t)$ and $s_Q^n(t)$, respectively, the outputs from all transmit filters are summed together to form the *m*-CAP signal, which is given by [16]

$$s(t) = \sum_{n=1}^{m} \left(s_I^n(t) \otimes f_I^{\,n}(t) - s_Q^n(t) \otimes f_Q^{\,n}(t) \right), \tag{4}$$

where $f_I^{\,n}(t)$ and $f_Q^{\,n}(t)$ are the in-phase and quadrature transmit filters, respectively, and $\otimes$ denotes the time domain convolution. The spectrum of $s(t)$ for $m = \{1, 2, 5\}$ is shown in Fig. 2. As can be seen, by increasing m the bandwidth assigned to each subcarrier becomes narrower, hence SCs within the 3-dB modulation bandwidth of the LED f_{LED}, are more robust against frequency-selectivity due to the limited

f_{LED}. However, this improvement is achieved at the cost of increased system complexity of *m*-CAP [4].

As illustrated in Fig. 1, at the Rx the input of *m*-CAP demodulator is split and applied to a set of matched filters $g_I^n(t)$ and $g_Q^n(t)$ in order to separate the in-phase and quadrature components, respectively. Following down-sampling and demodulation, *M*-QAM symbols are recovered and the received bits are compared with the transmitted bit stream in order to determine the BER [15].

2.2. VLC subsystem

Due to the limited bandwidth of LEDs, which hinders achieving higher data rates, pre-equalisation has been used as in [17]. Fig. 3 shows the frequency responses of the LED with and without a pre-equaliser, where f_{LED} is almost doubled with pre-equalisation. In indoor environments, multiple LED-based lighting fixtures are used to provide sufficient illumination levels, which facilitate the implementation of MIMO VLC. Let us consider the general case of a MIMO architecture with N_T Txs and N_R Rxs, with the line of sight (LOS) propagation paths. Hence, the $N_R \times N_T$ optical channel matrix is given by [10, 18]

$$\mathbf{H} = \begin{pmatrix} h_{11} & h_{12} & \cdots & h_{1N_t} \\ h_{21} & h_{22} & \cdots & h_{2N_t} \\ \vdots & \vdots & \ddots & \vdots \\ h_{N_r1} & h_{N_r2} & \cdots & h_{N_rN_t} \end{pmatrix}, \quad (5)$$

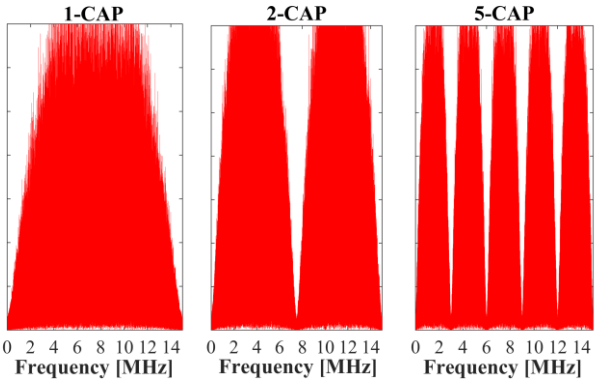

Fig. 2. *Frequency spectrum of s(t) for m = {1, 2, 5}*

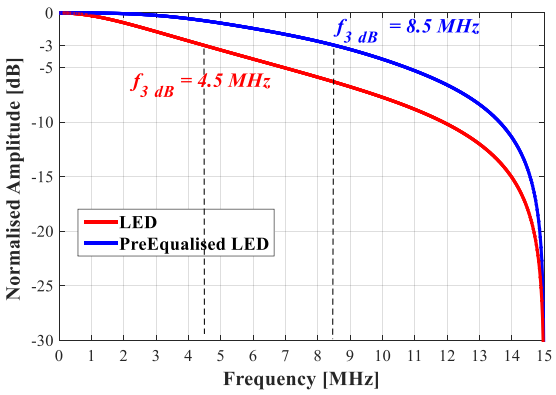

Fig. 3. *LED frequency response with and without a pre-equaliser*

where h_{ij} represents the channel gain between the i^{th} photodiode (PD) and j^{th} LED, which is given by

$$h_{ij} = \begin{cases} \dfrac{(L+1)A}{2\pi d^2}\cos^L(\phi)T_s(\psi)\cos(\psi), & 0 \le \psi \le \psi_c \\ 0, & \psi > \psi_c \end{cases}, \quad (6)$$

where $L = -\ln 2 / \ln(\cos(\phi_{1/2}))$ is Lambertian order and $\phi_{1/2}$ is the Tx's semi-angle. ϕ and ψ are the radiant and incident angles, respectively. *A* and ψ_c denote the surface area and field of view (FOV) of the PD, respectively. *d* is the distance between the i^{th} Rx and the j^{th} Tx, and $T_s(\psi)$ is the optical filter gain [19]. The adopted key system parameters are summarised in Table 1.

2.3. SISO m-CAP system

Fig. 4 shows the SISO *m*-CAP VLC system. At first, binary data stream is generated and passed through the *m*-CAP modulator, as depicted in Fig. 1. The *m*-CAP signal , which is DC-biased, is applied to a pre-equaliser prior to intensity modulation (IM) of the LED. The equaliser is employed to increase the system bandwidth beyond f_{LED} in order to increase the data transmission rate. Then after passing through the LED and indoor VLC channel, additive white Gaussian noise (AWGN) is added to the received signal. Following transmission through the wireless channel, the optical signal is then detected using an optical Rx, which is composed of a photodetector and a transimpedance amplifier. Having removed the DC level, a second equaliser is used the output of which is applied to the *m*-CAP demodulator in order to recover the transmitted data stream.

Table 1 System Parameters

Symbol	Parameter	Value
	Room size	5 m ×5 m ×3 m
h	Receiver height	85 cm
$\varphi_{1/2}$	Semi-power half angle	70°
FOV	PD field of view	60°
A	PD detector area	1 cm^2
R	Responsivity of PD	0.54 A/W
f_{LED}	LED cut-off frequency	4.5 MHz
	LED position for SISO structure	(1.8, 2.5, 3)
	PD position for SISO structure	(1.7, 2.5, 0.85)
	LED position for MIMO structure	(1.8, 2.5, 3) (3.2, 2.5, 3)
	PD position for MIMO structure	(1.7, 2.5, 0.85) (3.3, 2.5, 0.85)
m	Number of subcarriers	1, 2, 5, 8
B_{sub}	Subcarrier bandwidth	15, 7.5, 3, 1.875 MHz
β	Roll-off factor	0.5
L_f	Filter length	10 symbols
	Modulation type	QAM
M	Modulation order	2, 4, 8, 16, 32, 64

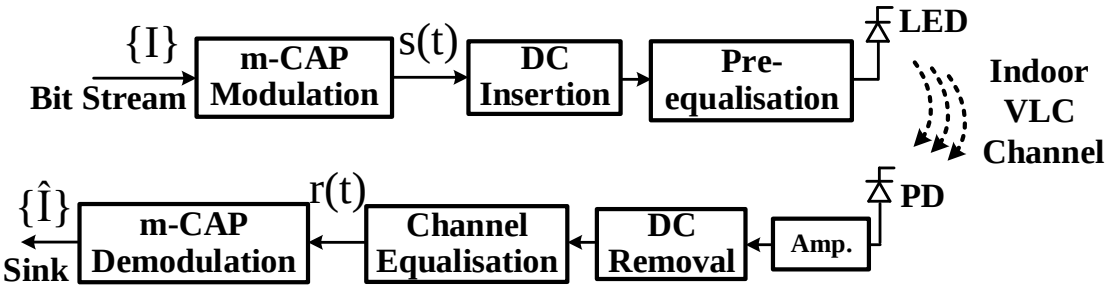

Fig. 4. *Block diagram of SISO m-CAP system*

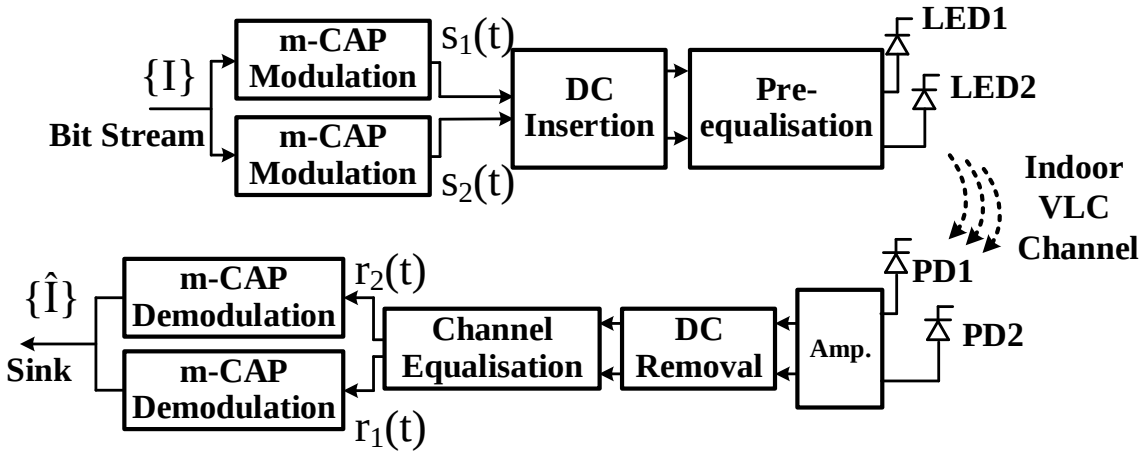

Fig. 5. *Block diagram of multiplexing MIMO m-CAP system*

2.4. Multiplexing MIMO m-CAP system

Fig. 5 illustrates the multiplexing MIMO scheme for the *m*-CAP VLC system. In this case, two independent data streams are applied to the *m*-CAP, the output of which is DC-level shifted and pre-equalised prior to IM of two light sources. This scheme offers an improved data rate compared to SISO. At the receiver, following transmission through the channel with a matrix **H**, the regenerated signal is passed through DC level and equaliser modules. Finally, the data streams are recovered using the *m*-CAP demodulators.

2.5. Spatial modulation for m-CAP system

Fig. 6 depicts the block diagram of the SM based *m*-CAP VLC system. First, the input bit stream is separated into blocks of size b_1, b_2, …, b_m for the 1st, 2nd, …, m^{th} SCs, respectively. Since two LEDs are used in this scenario, the first bit of each block represents the active LED. Strictly speaking, if the first bit in a data block is '**0**', then LED 1 is activated; otherwise LED 2 is used. The remaining bits in each block is converted into a QAM symbol by Gray mapping and assigned to the corresponding active LED.

In Fig. 7, all possible combinations of bits are shown for a 2-CAP SM with two Txs. The first bit in each block shows the active LED. The constellation size for 1st and 2nd SCs are 32 and 4, respectively. Therefore, the size of blocks for 1st and 2nd SCs are 6 and 3, respectively (i.e., $\log_2(M \times N_T)$). Also shown is an example of a random binary stream for better illustration of the process. First, the sequence is split into blocks of 6 and 3 bits for 1st and 2nd SCs, respectively. For the 1st subcarrier, the binary sequence is '**101111**', where for the first bit of '**1**' LED 2 is activated. The remaining bits of '**01111**' are converted to a complex symbol -1-3i by Gray mapping, which is inserted in the first slot of the vector $X_2(n)$. Simultaneously, the first slot of $X_1(n)$ is set to zero. Note, '**001**' represent the 2nd subcarrier. Thus, the complex QAM symbol -1-1i is assigned to LED 1 and is inserted in the second slot of the vector $X_1(n)$. At the same time, the second slot of $X_2(n)$ is set to zero. As shown in Fig. 6, $X_1(n)$ and $X_2(n)$ (i.e., outputs of spatial modulator) are passed through an *m*-CAP modulator, DC-bias, and pre-equaliser modules prior to IM of two LEDs.

At the Rx, following optical to electrical conversion and DC removal a zero forcing (ZF) equaliser is used to compensate for the deterioration of the MIMO VLC channel. Then the two output vectors corresponding to each row will be applied to the respective *m*-CAP demodulator. The resulting complex QAM symbols at the output of *m*-CAP demodulators are defined as $X'_1(n)$ and $X'_2(n)$. Afterward, the spatial demodulator estimates the index of the active LED by comparing the absolute value of the corresponding subcarrier as given by

$$\tilde{j}(n) = \arg\max_i \left(|X'_i(n)|\right), \quad i = 1, 2. \tag{7}$$

For instance, if $\tilde{j}(n)$ is equal to one, LED 1 is activated and if estimation is two then LED 2 is used for data transmission. The detected symbol corresponds to the maximum value in each case, which is given by

$$X'_d(n) = \begin{cases} X'_1(n), & \tilde{j}(n) = 1 \\ X'_2(n), & \tilde{j}(n) = 2 \end{cases}, \tag{8}$$

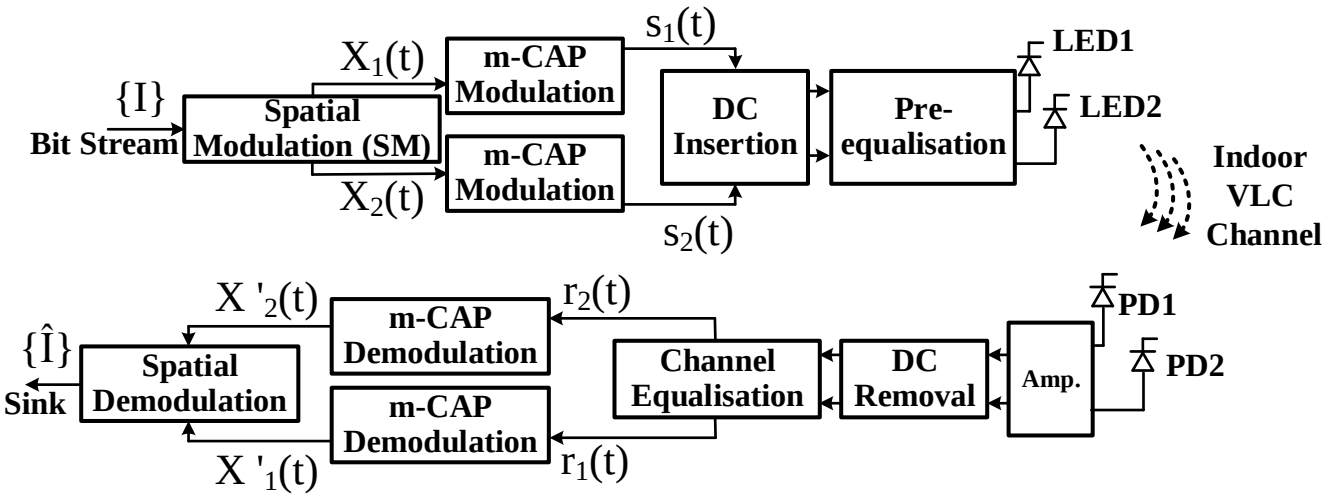

Fig. 6. *Block diagram of SM based m-CAP system*

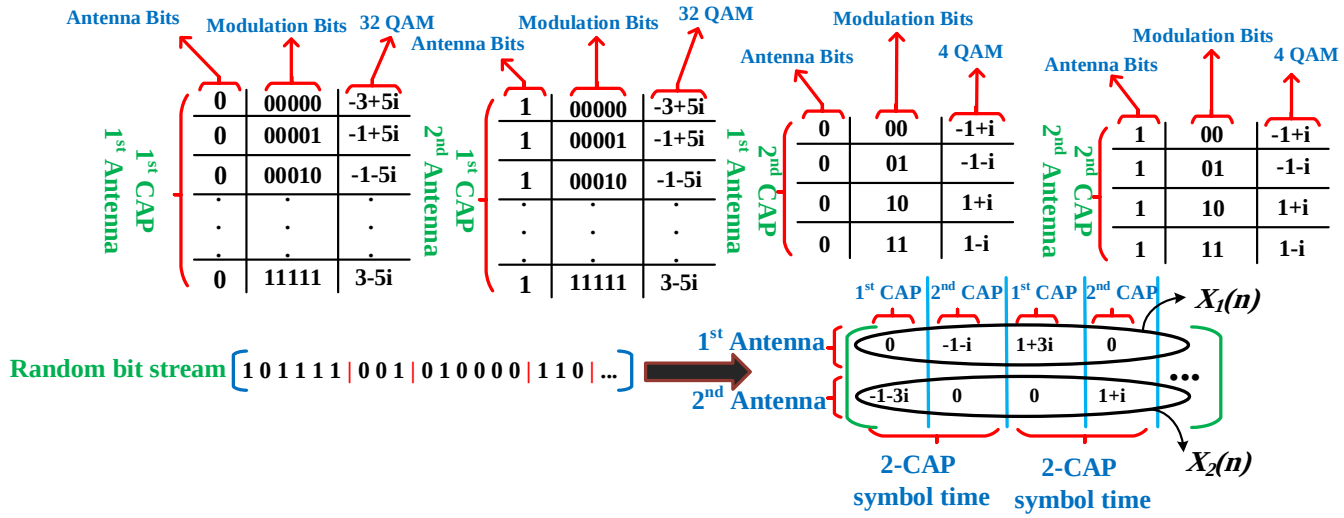

Fig. 7. *A schematic example of SM for 2-CAP system*

2.6. Non-DC m-CAP system

Fig. 8 shows the non-DC *m*-CAP structure for the VLC system. In order not to use a DC-bias, in non-DC *m*-CAP two LEDs are employed to transmit the positive and negative signals. For the positive signal the first LED is used whereas for the negative signal its absolute value is used for IM of the second LED. Note the use of pre-equalisation here too. At the Rx side, the outputs of equaliser are combined and then applied to the *m*-CAP demodulator, see Fig. 1. It is emphasised that, at any given time only one LED is active.

3. Simulation results

In this section, the BER and η_{se}/bitrate of the two proposed systems of SM and non-DC *m*-CAP, are investigated and compared along with the SISO and multiplexing MIMO *m*-CAP.

3.1. 1-CAP

Fig. 9 shows the BER performance as a function of the energy to noise ratio (E_b/N_0) for the post- and pre-equaliser based 1-CAP SISO system. Clearly, the ZF pre-equaliser based system offers improved BER performance. For instance, at the target BER of 10^{-3}, which is just below the forward error correction limit of 10^{-3}, there is an E_b/N_0 penalty of ~ 11 dB for post-equalisation compared to the pre-equalisation. This considerable difference is due to the noise enhancement of the post-equaliser. Hence, only pre-equalisation is considered from now one. In Fig. 10, the BER performance for different system setups for SISO and MIMO 1-CAP is compared. Also shown is the received constellation diagram for SISO at E_b/N_0 = 30 dB. Clearly, it can be seen that, non-DC 1-CAP outperforms others. For example, at a BER of 10^{-3} the E_b/N_0 penalties are 4.5, 6.6, and 10 for SM, SISO and multiplexing MIMO, respectively, compared with the non-DC *m*-CAP. This is due to the power efficiency of non-DC *m*-CAP, since negative valued signals are transmitted using the second LED without using a DC-bias.

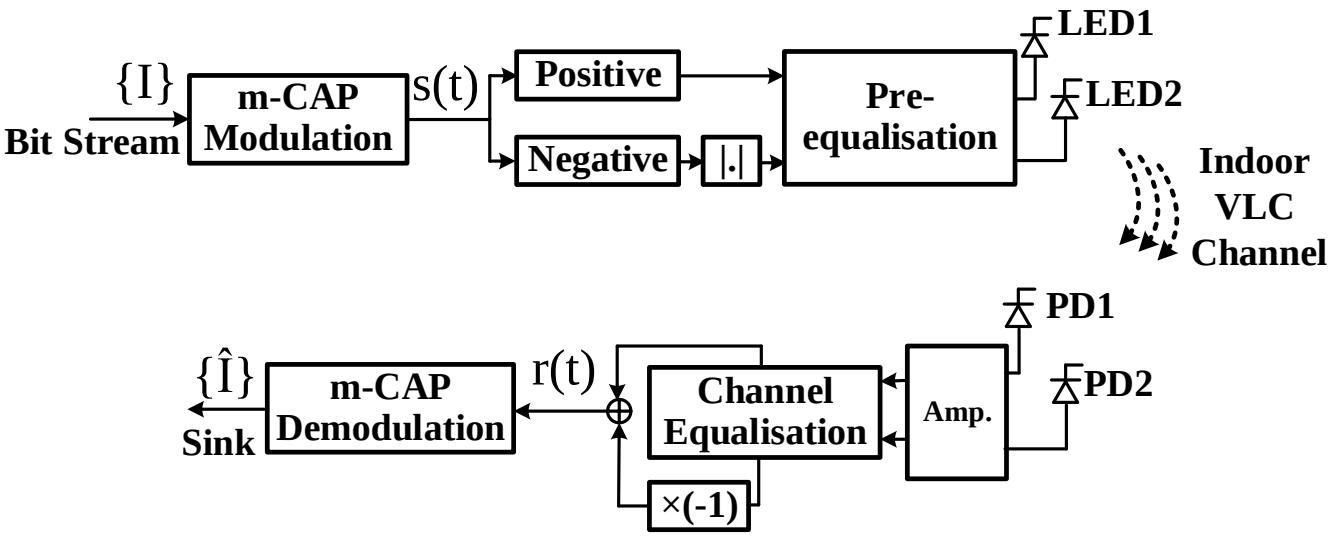

Fig. 8. *Block diagram of non-DC m-CAP system*

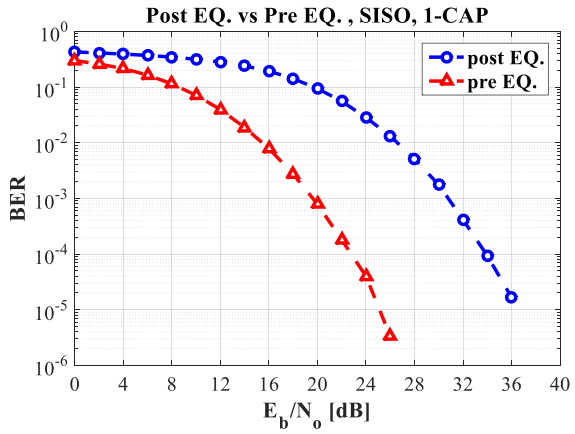

Fig. 9. *BER performance comparison of post-equaliser and pre-equaliser for 1-CAP SISO system*

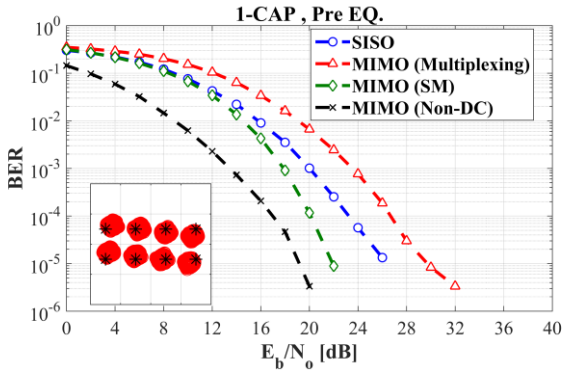

Fig. 10. *BER performance comparison of SISO, multiplexing MIMO, SM and non-DC 1-CAP systems*

3.2. 2- and 5-CAP

In Figs. 11 and 12, the BER performance of SISO, multiplexing MIMO, SM and non-DC 2-CAP are shown for 1st and 2nd SCs, respectively. The received constellation diagram of SISO at E_b/N_0 = 30 dB are also shown inset in figures. As illustrated in Fig. 11, the best BER performance is achieved by the non-DC 2-CAP with others incurring higher E_b/N_0 in order to deliver the same BER. For example, at a BER of 10^{-3} the power penalties in E_b/N_0 are ~ 7 dB, 8 and 12 dB, for MIMO (SM), SISO and MIMO (multiplexing), respectively, compared with MIMO (non-DC). A similar pattern is also in Fig. 12. Fig. 13 depicts the average BER of all SCs for 5-CAP non-DC, SM, SISO and multiplexing MIMO systems. Obviously, the superiority of non-DC 5-CAP over other schemes can be seen. For instance, the BER plot of non-DC 5-CAP reaches the target BER of 10^{-3} at E_b/N_0 = 13.2 dB, while for SM, SISO and multiplexing MIMO the corresponding E_b/N_0 values are 17.6, 20 and 23.5 dB, respectively.

3.3. Bitrate and spectral efficiency

Fig. 14 shows the bitrate and η_{se} for SISO, multiplexing MIMO, SM and non-DC *m*-CAP for $m = \{1, 2, 5, 8\}$. It can be seen that, multiplexing MIMO-based *m*-CAP outperforms others in terms of the bitrate and η_{se} for all values of *m*. For instance, for m = 2 the maximum bitrate of multiplexing MIMO is 70 Mbps, while for SISO, SM and non-DC the values are 35 Mbps, 45 Mbps and 35 Mbps, respectively. The corresponding η_{se} for these cases for m = 2 are 4.7 b/s/Hz, 2.3 b/s/Hz, 3 b/s/Hz and 2.3 b/s/Hz, respectively. Furthermore, for all scenarios both the bitrate and η_{se} are enhanced by increasing *m*. This is due to the use of bit loading, which assigns different number of bits to each subcarrier. By increasing *m*, bandwidth of each subcarrier becomes narrower, hence larger number of SCs within the 3-dB cut-off frequency of the pre-equalised LED will experience approximately flat subchannel. Thus, larger number of QAM orders can be assigned to these SCs, which improve the total bitrate. However, this improvement is not noticeable for larger values of *m*.

Finally, Fig. 15 illustrates the spectral efficiency against the target BER for 5-CAP. As shown, the spectral efficiency increases by increasing the target BER. In fact, higher modulation orders can be used by increasing the target BER, and thus higher spectral efficiencies can be achieved.

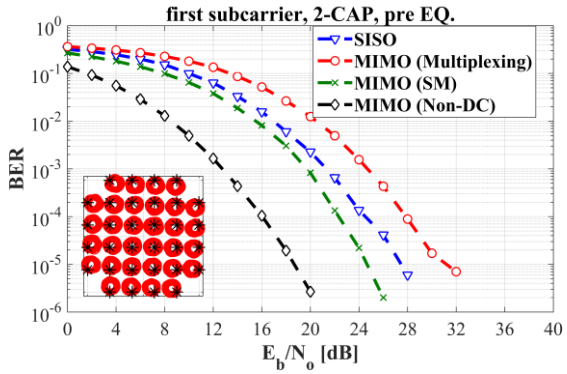

Fig. 11. *BER performance comparison of SISO, multiplexing MIMO, SM and non-DC 2-CAP systems for the 1st subcarrier*

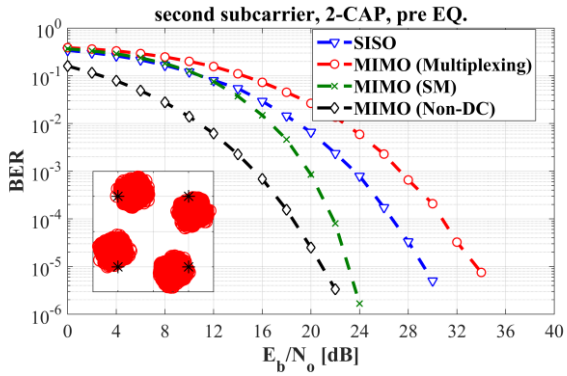

Fig. 12. *BER performance comparison of SISO, multiplexing MIMO, SM and non-DC 2-CAP systems for the 2nd subcarrier*

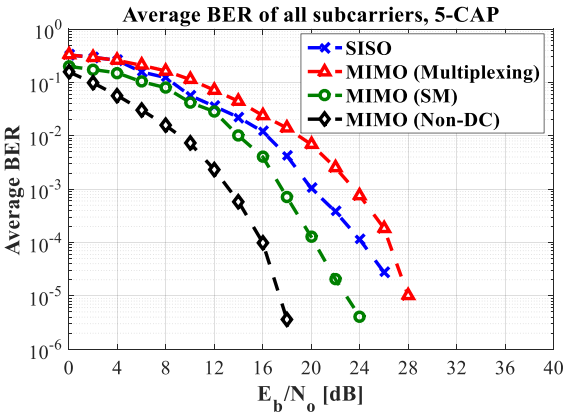

Fig. 13. *Average BER of all SCs for SISO, multiplexing MIMO, SM and non-DC 5-CAP systems*

4. Conclusion

In this paper, the SM and non-DC techniques for *m*-CAP VLC systems were investigated for the first time. The results for these systems were compared with the SISO and multiplexing MIMO *m*-CAP systems in terms of the BER performance and the spectral efficiency for different orders of *m*. BER plots for $m = \{1, 2, 5\}$ demonstrated the superiority of non-DC *m*-CAP over other techniques. This is due to the power efficiency of non-DC *m*-CAP since positive and negative signals are sent by LED 1 and LED 2, respectively, and no DC-bias is required. SM for *m*-CAP is the next option which performs better than SISO and multiplexing MIMO *m*-CAP systems in terms of BER. Furthermore, spectral efficiency and bitrate for SISO, multiplexing MIMO, SM and non-DC *m*-CAP were carried out for $m = \{1, 2, 5, 8\}$. It was shown that multiplexing MIMO *m*-CAP achieves higher bitrate or spectral efficiency compared with other techniques for all values of *m*, since two LEDs were used to transmit separate data streams. In addition, the proposed SM *m*-CAP is the next choice to obtain higher bitrate compared to SISO and non-DC MIMO *m*-CAP, because it exploits both spatial and signal domain constellations. As the results showed, there is a trade-off between the BER performance and the bitrate. For example, non-DC *m*-CAP is the best technique to obtain the best BER performance, however it achieves the same bitrate as the SISO *m*-CAP. On the other hand, the multiplexing MIMO *m*-CAP is the best choice in terms of bitrate, while its BER performance is the worst one. Among all of the investigated techniques, SM demonstrated a moderate performance for the BER and the spectral efficiency, thus it can be used for the applications in which reasonable bitrate and BER performance are required.

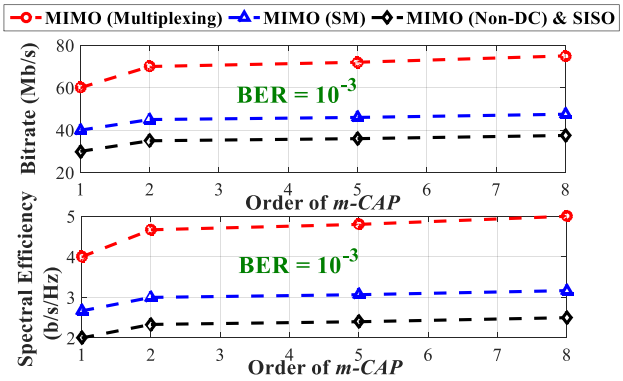

Fig. 14. *Bitrate (top pane) and spectral efficiency (bottom pane) of SISO, multiplexing MIMO, SM and non-DC m-CAP for m = {1, 2, 5, 8} at target BER of 10^{-3}*

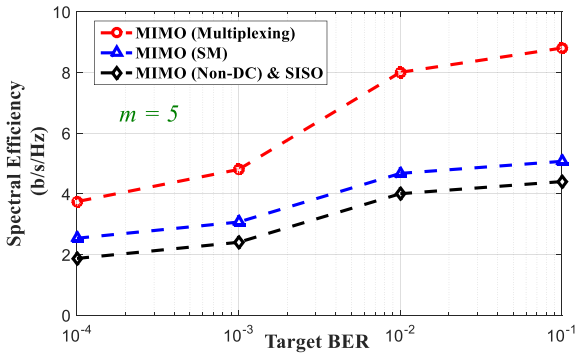

Fig. 15. *Spectral efficiency against the target BER for 5-CAP*

5. References

[1] Karunatilaka, D., Zafar, F., Kalavally, V., *et al.* 'LED based indoor visible light communications: state of the art', *IEEE communications surveys and tutorials*, 2015, 17, (3), pp. 1649-1678.

[2] Ghassemlooy, Z., Alves, L. N., Zvanovec, S., *et al. Visible light communications: theory and applications*, (CRC Press, 2017)

[3] Wu, F. M., Lin, C. T., Wei, C. C., *et al.* '1.1-Gb/s white-LED-based visible light communication employing carrier-less amplitude and phase modulation', *IEEE photonics technology letters*, 2012, 24, (19), pp. 1730-1732.

[4] Haigh, P. A., Le, S. T., Zvanovec, S., *et al.* 'Multi-band carrier-less amplitude and phase modulation for bandlimited visible light communications systems', *IEEE Wireless Communications*, 2015, 22, (2), pp. 46-53.

[5] Wu, F. M., Lin, C. T., Wei, C. C., *et al.* 'Performance comparison of OFDM signal and CAP signal over high capacity RGB-LED-based WDM visible light communication', *IEEE Photonics Journal*, 2013, 5, (4), pp. 7901507-7901507.

[6] Haigh, P. A., Burton, A., Werfli, K., *et al.* 'A multi-CAP visible-light communications system with 4.85-b/s/Hz spectral efficiency', *IEEE Journal on Selected Areas in Communications*, 2015, 33, (9), pp. 1771-1779.

[7] Olmedo, M. I., Zuo, T., Jensen, J. B., *et al.* 'Multiband carrierless amplitude phase modulation for high capacity optical data links', *Journal of Lightwave Technology*, 2014, 32, (4), pp. 798-804.

[8] Haigh, P. A., Chvojka, P., Zvanovec, S., *et al.* 'Experimental verification of visible light communications based on multi-band CAP modulation', in *Optical Fiber Communication Conference*, (Optical Society of America, 2015)

[9] Akande, K. O. and Popoola, W. O., 'MIMO techniques for carrierless amplitude and phase modulation in visible light communication', *IEEE Communications Letters*, 2018, 22, (5), pp. 974-977.

[10] Werfli, K., Chvojka, P., Ghassemlooy, Z., *et al.* 'Experimental demonstration of high-speed 4×4 imaging multi-CAP MIMO visible light communications', *Journal of Lightwave Technology*, 2018, 36, (10), pp. 1944-1951.

[11] Mesleh, R., Elgala, H., and Haas, H., 'Optical spatial modulation', *IEEE/OSA Journal of Optical Communications and Networking*, 2011, 3, (3), pp. 234-244.

[12] Fath, T., Haas, H., Di Renzo, *et al.* 'Spatial modulation applied to optical wireless communications in indoor LOS environments', in *GLOBECOM 2011*, (2011)

[13] Li, Y., Tsonev, D., and Haas, H., 'Non-DC-biased OFDM with optical spatial modulation', in *Personal Indoor and Mobile Radio Communications (PIMRC), 2013 IEEE 24th International Symposium on*, (IEEE, 2013)

[14] Chvojka, P., Haigh, P. A., Zvanovec, S., *et al.* 'Evaluation of multi-band carrier-less amplitude and phase modulation performance for VLC under various pulse shaping filter parameters', in *OPTICS*, (2016)

[15] Chvojka, P., Werfli, K., Zvanovec, S., *et al.* 'On the m-CAP performance with different pulse shaping filters parameters for visible light communications', *IEEE Photonics Journal*, 2017, 9, (5), pp. 1-12.

[16] Zhang, J., Yu, J., Li, F., *et al.* '11×5×9.3 Gb/s WDM-CAP-PON based on optical single-side band multi-level multi-band carrier-less amplitude and phase modulation with direct detection', *Optics express*, 2013, 21, (16), pp. 18842-18848.

[17] Nassiri, M., Ashouri, S., Baghersalimi, G., *et al.* 'A comparative performance assessment between pre-equalization and post-equalization techniques in m-CAP indoor VLC systems with bit loading', in *First West Asian Colloquium on Optical Wireless Communications (WACOWC2018)*, (2018)

[18] Rajbhandari, S., Chun, H., Faulkner, G., *et al.* 'Imaging-MIMO visible light communication system using μLEDs and integrated receiver', in *Globecom Workshops (GC Wkshps), 2014*, (IEEE, 2014)

[19] Tran, N. A., Luong, D. A., Thang, T. C., *et al.* 'Performance analysis of indoor MIMO visible light communication systems', in *Communications and Electronics (ICCE), 2014 IEEE Fifth International Conference on*, (IEEE, 2014)